2024 IEEE/RSJ International Conference on Intelligent Robots and Systems (IROS)
October 14-18, 2024. Abu Dhabi, UAE

A Novel Geometrical Structure Robot Hand for Linear-parallel Pinching and Coupled Self-adaptive Hybrid Grasping

Shi Chen, Bihao Zhang, Kehan Feng, Yizhou Wang, Jiayun Li and Wenzeng Zhang, Member, IEEE

***Abstract*— Current robot hand grippers capable of self-adaptive or coupled grasping often cannot perform linear-parallel pinching at the physical end of the gripper, which is widely used in industrial applications. For this reason, this paper introduces a gripper with hybrid grasping modes— the LPCSA hand. It can achieve three grasping modes: linear-parallel pinching, coupled, and self-adaptive grasping. The design cleverly couples two kinds of Chebyshev linear mechanisms to enable flat movement at the end of the finger. It also utilizes the deformability of the parallelogram to achieve self-adaptive grasping. Furthermore, the gripper uses an idle stroke and a special component to facilitate the switch between the three modes. The linear-parallel pinching function is suitable for pinching objects of different sizes on the desktop. The self-adaptive grasping mode can adapt to objects of various shapes and sizes. The coupled grasping mode enables fast grasping of irregular objects. This paper also analyzes the kinematics and dynamics of the LPCSA hand. Combined with experiments, it demonstrates that the LPCSA hand has a wide range of grasping space and stable performance.**

I. INTRODUCTION

The robot hand, as a key device of the robot, is tasked with grasping, manipulating, and interacting with the outside world[1], so its design and performance are critical. Robot hands with less complex designs and fewer motors have been created to grasp objects securely, they are underactuated hand[2]. In 2004, Birglen[3] presented an analysis of self-adaptive underactuated grasping patterns and control theory. In 2007, Dollar[4] combines mechanical design and machining to propose the SDM hand, a underactuated robot hand with four fingers.

As the research on underactuated fingers continues to deepen, underactuated fingers capable of performing multiple functions have been proposed. The coupled hand was developed to behave like the human hand, where the phalanxes can touch objects almost simultaneously[5]. The coupled and self-adaptive mode (called COSA mode) was further proposed[6] and coupled and self-adaptive hands (such as CDSA hand[7], COSA-E hand, etc.) were developed.

Shi Chen is with Nanchang University, Nanchang, China and X-Institute, Shenzhen, China (e-mail: cs749545305@163.com)

Bihao Zhang is with the University of Science and Technology of China, Hefei, China (e-mail: dadaizibi@mail.ustc.edu.cn)

Kehan Feng is with Changkong College, Nanjing University of Aeronautics and Astronautics, Nanjing, China (e-mail: fengkehan@nuaa.edu.cn)

Yizhou Wang is with the Southern University of Science and Technology, Shenzhen, China (e-mail: 12312603@mail.sustech.edu.cn)

Jiayun Li is with the Hong Kong University of Science and Technology, Shenzhen, China (e-mail: lijiayun1220@outlook.com)

Wenzeng Zhang is with X-Institute, Shenzhen, China and Department of Mechanical Engineering, Tsinghua University, Beijing, China (corresponding author to provide zhangwenzeng@x-institute.edu.cn)

In order to take advantage of the human-like pinching and industrial grippers, the parallel and self-adaptive grasping mode (called PASA mode) was proposed[8]. Since such parallel grasping ends usually appear to have curved trajectories and are not suitable for gripping fine objects[9], various robot hands or fingers with linear-parallel self-adaptive grasping mode was proposed. These linear-parallel grasping modes can be realized with mechanisms such as Chebyshev linkage[10], Y-shaped linkage[11] and Hoeckens Mechanism[12]. On the basis of all this, there are also many fingers and hands that combine some of the functions of self-adaptive, coupling, parallel grasp and linear-parallel pinching, and propose a hybrid grasping mode that can be switched in different situations, like the SCHU hand[13] and the LIPSA hand[14].

This paper presents a linear-parallel coupled self-adaptive (LPCSA) robot hand (figure 1) featuring a three-joint mechanism based on a novel Chebyshev linkage mechanism, characterized by the combination of an common Chebyshev mechanism and a Hoechen linkage mechanism. The proposed mechanism enables hybrid grasping, allowing for switching between linear-parallel and coupled grasping modes. The paper analyzes the functionality, grasping methods, movement, and forces involved in the design. To validate the analysis, a prototype was manufactured.

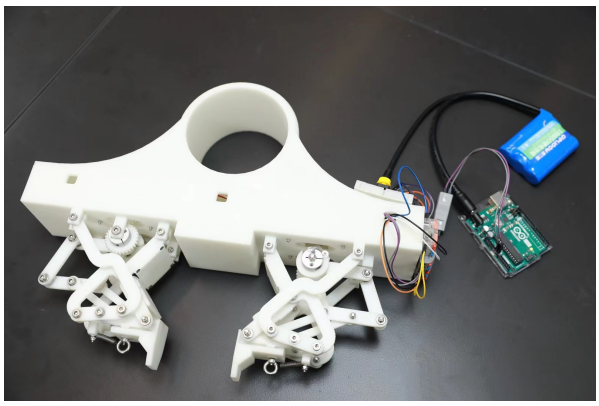

Fig. 1: LPCSA hand devices.

II. DESIGN OF THE LPCSA HAND

The LPSCA Hand is composed of two fingers placed symmetrically. The working principles of a single finger will be explained in the following sections.

A. Composition of the LPCSA Hand

The finger is mainly composed of two mechanisms, as shown in figure 2: A Chebyshev Translating Table Linkage (CTTL), and a Double Parallelogram Mechanism (DPM). The parts associated with grasping are Finger Segment 1 (FS1), Finger Segment 2 (FS2), Finger Base (FB), Finger Tip (FT). FB and FT are joined at Rotary Joint 1 (RJ1), allowing FT to move with FB and tilt in respect to it. The rings on FB and FT are joined by Extension Spring (ES), ensuring that when unactuated, FT is parallel to FB. Drive Bar 1 (DB1) and Drive Bar2 (DB2) of DPM are actuated by drive wheels. CTTL (which combines two straight-line mechanisms: the Chebyshev Linkage and the Hoecken Linkage) ensures the linear-parallel motion of FB, and DPM is used to tilt FT for self-adaptation.

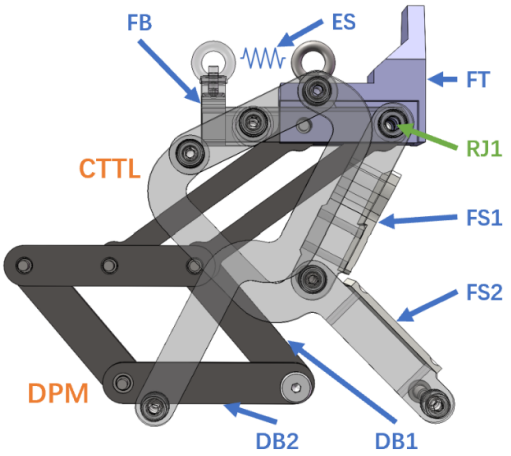

Fig. 2: Core mechanisms of the LPCSA Finger. CTTL is turned transparent and DPM is set as opaque. FS1, FS2 and FB belong to CTTL while FT, DB1, DB2 belong to DPM, as shown. FT and FB are jointed at RJ1. ES is not modelled and is drawn in the figure instead.

The finger has two types of motion, as shown in figure 3: The linear motion of FB, resulting from Drive Wheel 1 (DW1) actuating DB1, and the tilting motion of FT, resulting from Drive Wheel 2 (DW2) actuating DB2. DW1 and DW2 are rigidly attached onto the Drive Shaft (DS). Actuating the finger refers to the motor driving DS through a gear set.

As shown in figure 4. DW1 drives DB1 through a Torsion Spring (TS), with a Limiting Block (LB) constraining DB1's forward motion. Meaning that if the finger contacts an object, CTTL stops moving, but due to the spring, DW1 (along with DW2) can continue to rotate for the rest of the action to take place.

As shown in figure 5. DW2 drives DB2 through a drive block. There are two slots for inserting the drive block, and its choice controls the idle stroke of tiling relative to linear motion: Slot 1 means that tilting only begins after linear motion, Slot 2 results in tilting along with linear motion. In effect, the slot choice decides whether tilting is decoupled from or coupled to the linear motion.

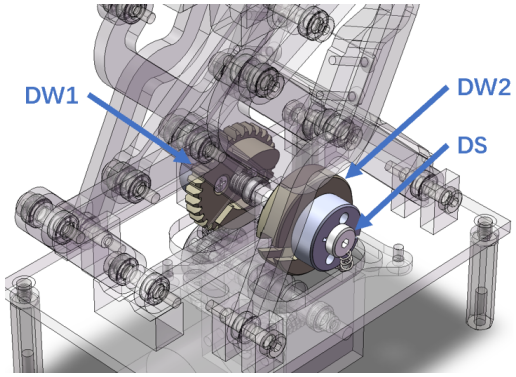

Fig. 3: Driving mechanisms of the LPCSA Finger. DW1, DW2 and DS are shown as opaque. DS is shown as a bold screw.

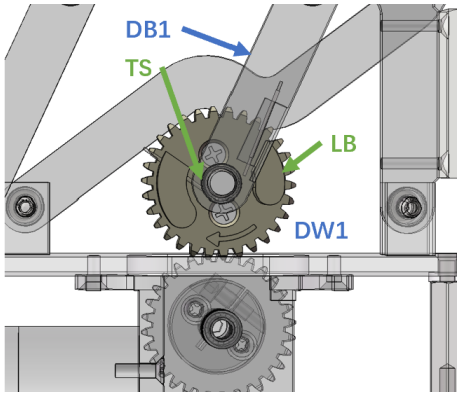

Fig. 4: Close-up of DW1. TS, LB and DB1 are shown.

B. Working Principle of the LPCSA Hand

The finger has three types of grasping modes: Linear-Parallel Pinching (LPP), Linear-Parallel Self-Adaptive Grasping (LPSAG), and Coupled Grasping (CG). The working principle is explained as follows. The LPCSA finger Schematics are shown in figure 6 and the grasping modes are shown in figure 7.

For LPP and LPSAG, DW2 is set to slot 1. When the finger is actuated, FB (along with FT) moves forward in a linear-parallel fashion. When the finger contacts an object, CTTL stops but DS continues to be actuated. When DS turns enough for DW2 to start actuating DB2, FT attempts to tilt. If FT is already in contact with the object, then it remains parallel to FB, pinching the object (LPP). If FT is not in contact, then it tilts until contacting the object, resulting in a better adaptation to the object's shape, achieving self-adaptive grasping (LPSAG).

For CG, DW2 is set to slot 2. When the finger is actuated, FT tilts along with the forward motion, and the finger stops upon contact with an object, completing the grasp. Without waiting for the idle stroke to complete, CG finishes grasping more quickly than LPSAG.

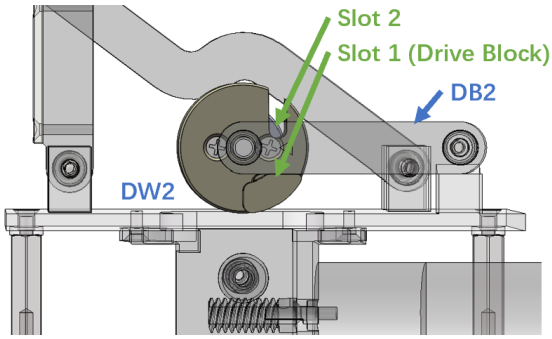

Fig. 5: Close-up of DW2. Slot 1, Slot 2, Drive Block and DB2 are shown. Drive Block is inserted in Slot 1.

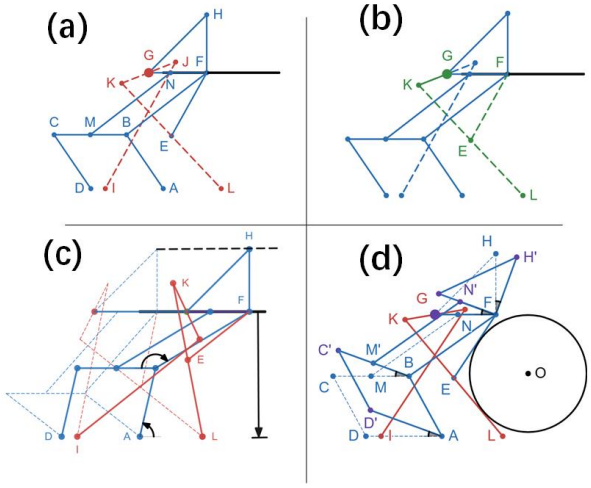

Fig. 6: LPCSA finger Schematics. (a) the red dashed line is Chebyshev mechinsm; (b) the green dashed line is Hoechen mechinsm; (c) linear-parallel pinching Schematic; (d) self-adaptive grasping Schematic.

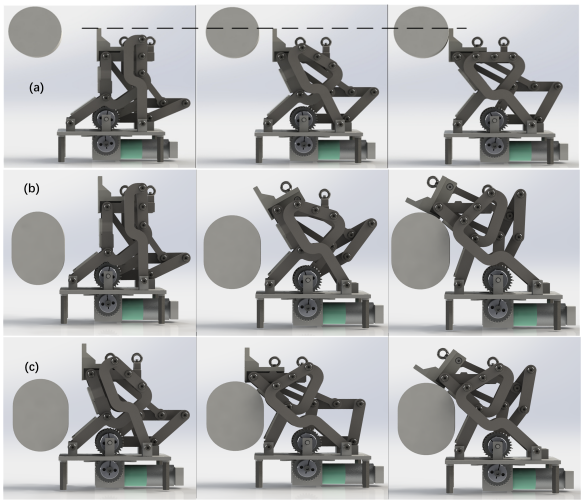

Fig. 7

III. Analysis of the LPCSA Finger

To investigate the performance characteristics of the LPCSA hand, we performed Kiematic analysis and grasping force analysis on a single LPCSA finger.

A. Kinematic Analysis of the LPCSA Hand

Firstly, a mathematical model of the robotic finger was established by representing the axle as a point and the rod as a line, as illustrated in Figure 8.

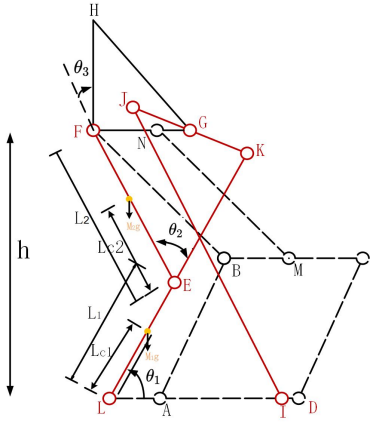

Fig. 8: Mathematical model.

Assuming that the reference coordinate system is established with each rotational joint of the finger as the origin, the D-H parameters for the mathematical model of the finger can be obtained, as follows:

TABLE I: Standard D-H Parameters for LPCSA Finger

link	α_i	a_i	d_i	θ_i
1	0	L_1	0	θ_1
2	0	L_2	0	θ_2

From the D-H table, the transformation matrix is:

$$A_i = \begin{bmatrix} \cos\theta_i & -\sin\theta_i & 0 & L_i\cos\theta_i \\ \sin\theta_i & \cos\theta_i & 0 & L_i\sin\theta_i \\ 0 & 0 & 1 & 0 \\ 0 & 0 & 0 & 1 \end{bmatrix} \tag{1}$$

The transformation matrix of the two rods are:

$$T_1^0 = A_1, T_2^o = A_1A_2 \tag{2}$$

Introduction of the Jacobi Matrix:

$$\xi = J\dot{\theta}, \xi = \begin{bmatrix} V_n^0 \\ W_n^0 \end{bmatrix}, J = \begin{bmatrix} J_v \\ J_w \end{bmatrix} \tag{3}$$

$$J_{vi} = Z_{i-1}^0 * (O_n - O_{i-1}), J_{wi} = Z_{i-1}^o \tag{4}$$

According to the above equation and combined with the kinematic simulation software, when the mechanism is driven by a uniform velocity, the motion characteristics of its fingertip can be known, as shown in figure 9.

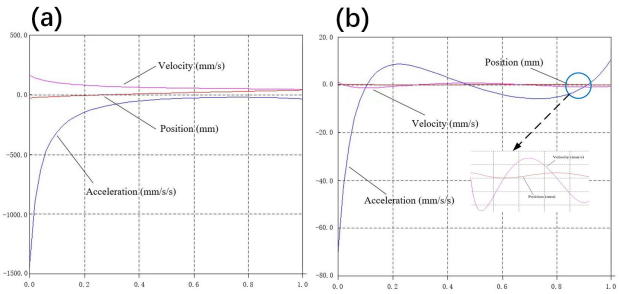

Fig. 9: Motion characteristic of the LPCSA hand. (a) horizontal kinematic characteristic of the mechanism; (b) vertical kinematic characteristic of the mechanism.

As shown in the diagram, here, we focused on the fingertip's motion, finding its movements are smooth except at the start from the x direction, ideal for fragile items like eggs; from the y direction, the displacement is approximately zero, which verifies the linear motion.

Combining the above kinematical equations using the Lagrangian method to derive the kinetic equations, the Jacobi matrix can be derived to find the velocity and angular velocity of the finger during motion and the kinetic energy of the rigid body:

$$K = \frac{1}{2} m v^T v + \frac{1}{2} \omega^T \omega \tag{5}$$

$$P = \sum_{i=1}^{2} P_i = (m_1 L_{c1} + m_2 L_1) g \sin\theta_1 + m_2 L_{c2} g \sin(\theta_1 + \theta_2) \tag{6}$$

Then substituting into the robot dynamics equations:

$$M(\theta)\ddot{\theta} + C\left(\theta, \dot{\theta}\right)\dot{\theta} + G(\theta) = \tau \tag{7}$$

In practical robotic hand design work, the results of the above equations can be used as a reference for mechanism design and optimization.

B. Grasping force analysis of the LPCSA Hand

In addition to the kinematic analysis, this subsection carries out the analysis of the static mechanics of the LPCSA finger, and the static model established based on the structure of the fingers and the corresponding physical meanings of the symbols are shown in figure 10 and the table.

TABLE II: Physical Symbols and Their Meanings

quantity	notation	unit
F_1, F_2, F_3	Grasping power of the first, second and third phalanxes.	N
L_1, L_2, L_3	Length of the first, second and third phalanxes.	mm
h_1, h_2, h_3	Vertical distance of the contact point of the first (second or third) phalanx from the proximal connection joint.	mm
G_1, G_2, G_3	Point of contact of the first (second or third) phalanx with the object.	mm
T	Torque transmitted by the actuator to the drive rod.	Nmm
k	Coefficient of strength of springs.	N/mm
$\theta_1, \theta_2, \theta_3$	Angle between the first, second and third phalanxes and the vertical direction.	rad

In the linear parallel grasping mode, as shown in figure 10(a), the coordinate system is established with point E as the coordinate origin. Since the first and second phalanxes only provide support, so as to simplify the analysis, only the grasping force of the fingertip is analyzed. According to the moment equilibrium condition the equation is obtained as:

$$T = F_3 * (h_3 + L_2 \cos\theta_2) \tag{8}$$

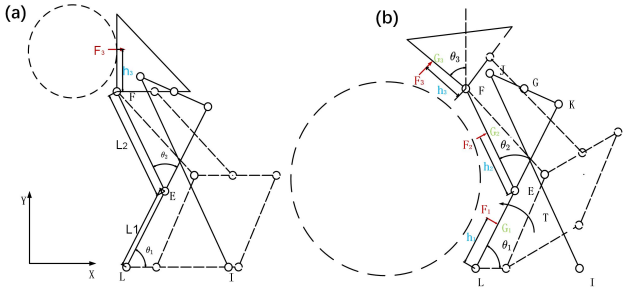

Fig. 10: Hydrostatic model. (a) linear-parallel pinching force analysis; (b) self-adaptive grasping force analysis.

Let T=20N*mm and L_2=70mm. From the equation, we can obtain the relationship with the grasping force and the the angle of rotation of the second finger segment or the hight of contact point, as shown in figure 11(a).

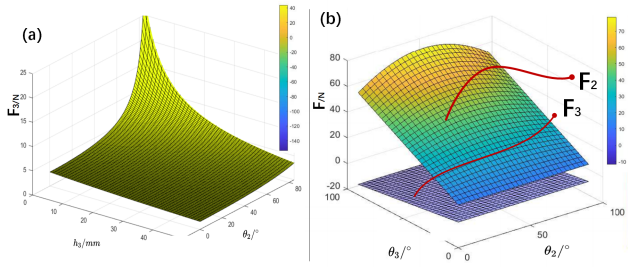

Fig. 11: Analysis on the grasp force. (a) parallel grasp stage; (b) self-adaptive grasp stage.

The LPCSA finger enters the self-adaptive grasping mode when the object comes into contact with the first phalanx or the second phalanx and obstructs the movement of the first phalanx or the second phalanx. To simplify the analysis, only analyze the grasping force of the second and third phalanxes. The force analysis in the self-adaptive grasping mode is shown in figure 11(b), in which the spring for limitation applies a moment in the opposite direction.

The vector expressions for the contact points of the two finger segments with the object are

$$\overrightarrow{F_2} = (F_2 \cos\theta_2, -F_2 \sin\theta_2) \tag{9}$$

$$\overrightarrow{F_3} = (F_3 \cos\theta_3, -F_3 \sin\theta_3) \tag{10}$$

The imaginary displacement of the contact point can be obtained:

$$\overrightarrow{G_1} = (h_1 \sin\theta_1, h_1 \cos\theta_1) \tag{11}$$

$$\overrightarrow{G_3} = (L_2 \sin\theta_2 + h_3 \sin\theta_3, L_2 \cos\theta_2 + h_3 \cos\theta_3) \tag{12}$$

According the Newton-Euler equations,

$$[T \ \ -k\theta_3]\begin{bmatrix} \delta\theta_2 \\ \delta\theta_3 \end{bmatrix} = \begin{bmatrix} \vec{F_2} & \vec{F_3} \end{bmatrix}\begin{bmatrix} \delta\vec{G_2} \\ \delta\vec{G_3} \end{bmatrix} \tag{13}$$

$$[T \ \ -k\theta_3] = [F_2 \ F_3]J \tag{14}$$

$$J = \begin{bmatrix} h_2 & 0 \\ L_2\cos(\theta_2-\theta_3) & h_3 \end{bmatrix} \tag{15}$$

$$F_2 = \frac{T}{h_2} + \frac{k\theta_3 L_2\cos(\theta_2-\theta_3)}{h_2 h_3}, F_3 = -\frac{k\theta_3}{h_3} \tag{16}$$

And J in Eq. (19) refer to the Jacobi matrix. According to Eq. (14-21), the relationship between each parameter and the grasping force can be obtained, as shown in Fig. 12(b).

We analyze the grasping force, displacement, and angle during linear gripping.In the parallel mode, the grasping force remains stable except at the start.In the adaptive mode, when θ_2 is near 50 degrees, the second segment's force increases, while the first segment's force is proportional to θ_3.

Additionally, we conducted a workspace analysis of the LPCSA hand. If a mechanism comprises numerous linkages, they will undoubtedly occupy a significant amount of space during operation, which will markedly reduce space efficiency. Therefore, this consideration was thoroughly addressed in the design of the LPCSA hand. As for its single finger, it utilizes 15 linkages (including equivalent linkages), two linear linkage mechanisms, and one parallelogram mechanism. We identified the optimal connection axis positions to maximize the overlap of each mechanism's workspace. As illustrated in Figure 12, blue area represents the workspace of the parallelogram mechanism and the fingertip, while red area represents the workspace of the two linear linkage mechanisms. Calculations reveal that the overlap area between blue area and red area accounts for 47.35 percent of the total area, indicating that our design significantly enhances the compactness of the LPCSA hand structure.

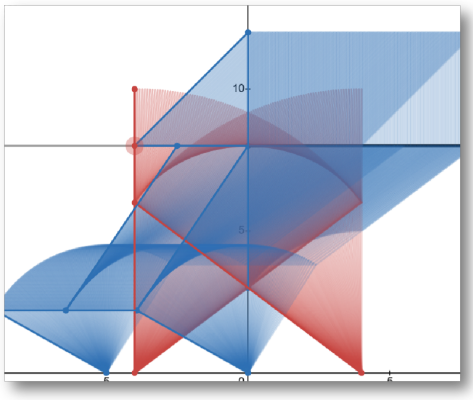

Fig. 12: Workspace analysis. Blue area represents the Workspace of the parallelogram mechanism and the fingertip;Red area represents the workspace of the two linear linkage mechanism.

IV. Experiments

In order to verify the feasibility of this LPCSA finger design, a prototype based on the it is made and grasping experiments are conducted. As shown in figure 13, the LPCSA finger has a linear-parallel grasping range of 0-80mm and a self-adaptive range of 0-90 degrees.

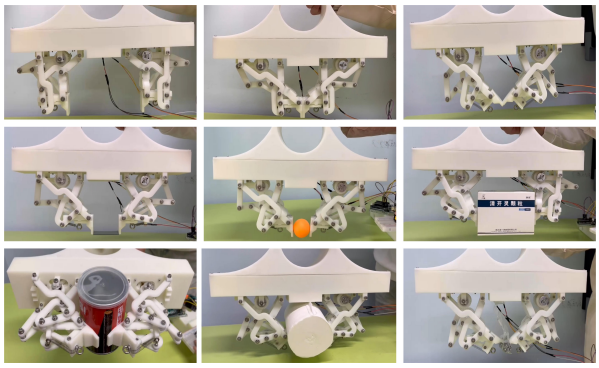

Fig. 13: LPCSA Finger Physical Grip.

This experiment used an FSR402 resistive thin film pressure sensor, installed at the end of the gripper's second joint, to fully touch objects. The sensor was in contact with both rigid and flexible objects, and the pressure changes over time were observed, as shown in figure 14. The experimental results indicate that the gripper exhibits different grasping strengths when in contact with objects of varying stiffness. In the experiment, the LPCSA hand demonstrated its ability to grasp objects of different stiffnesses, depend on the pinching mode experiment, primarily detecting the pressure changes at the fingertip of the second phalanx. For further development, it is suggested to consider placing a matrix of force sensors on both finger phalanxes to monitor the pressure changes throughout the entire process, ensuring accurate control.

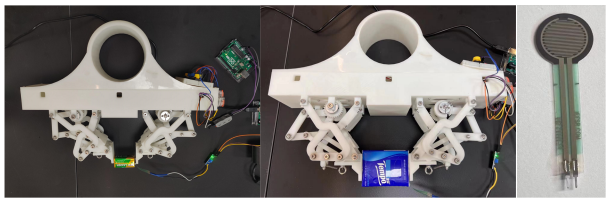

Fig. 14: Experimental device.

The other LPCSA finger is symmetrical to it, and the two fingers are combined to form the LPCSA gripper to grasp physical objects, as shown in Fig. 15. The LPCSA gripper allows three gripping modes, allowing objects of different sizes, shapes, and postures to be grasped with a single actuator. When it is necessary to grasp objects with high friction, an elastic material with a high coefficient of friction (rubber or silicone) can be added to the finger surface to improve the stability of the grasp.

V. CONCLUSIONS

In essence, mechanical systems generally consist of various parts (e.g., gears, racks, sliders, linkages). The unique

Fig. 15: The application of the gripper.

feature of the mechanical hand designed in this paper is its multi-link mechanism (with the worm and gear only for transmission). This simple and easy-to-implement mechanism, coupled with two linear mechanisms, stabilizes and enhances the flexibility of the fingers' linear-parallel pinching mode. The instability and deformability of the double parallelogram further improve this mode. The double parallelogram also increases the adaptive grasping range. The pure linkage mode mechanism operates at high speed, and the LPCSA fingers achieve smooth and substantial grasping force while maintaining rapid transmission. Its linear-parallel pinching capability allows it to grasp objects of different sizes, making it suitable for future applications in household humanoid robots for tasks like folding clothes or industrial robots. To improve the robot hand, precise control of finger segments still needs improvement through the application of sensors and control algorithms.

REFERENCES

[1] Billard, A., Kragic, D. (2019). Trends and challenges in robot manipulation. Science, 364(6446), eaat8414.

[2] Laliberté, T., and Gosselin, C. M. (1998). Simulation and design of underactuated mechanical hands. Mechanism and machine theory, 33(1-2), 39-57.

[3] Birglen L, Gosselin C. M. Kinetostatic analysis of underactuated fingers[J]. IEEE Transactions on Robotics and Automation, 2004, 20(2): 211-221.

[4] Dollar, A. M., and Howe, R. D. (2007, June). The SDM hand as a prosthetic terminal device: a feasibility study. In 2007 IEEE 10th International Conference on Rehabilitation Robotics (pp. 978-983). IEEE.

[5] Dubey, V. N., and Crowder, R. M. (2004, January). Grasping and control issues in adaptive end effectors. In International Design Engineering Technical Conferences and Computers and Information in Engineering Conference (Vol. 46954, pp. 327-335).

[6] Li, G., and Zhang, W. (2010, December). Study on coupled and self-adaptive finger for robot hand with parallel rack and belt mechanisms. In 2010 IEEE International Conference on Robotics and Biomimetics (pp. 1110-1115). IEEE.

[7] Liang, D., Zhang, W., and Xu, X. (2016, December). COSA-E hand: A coupled and self-adaptive hand with eccentric wheel mechanisms. In 2016 IEEE International Conference on Robotics and Biomimetics (ROBIO) (pp. 544-549). IEEE.

[8] Liang, D., Song, J., Zhang, W., Sun, Z., and Chen, Q. (2016). PASA hand: A novel parallel and self-adaptive underactuated hand with gear-link mechanisms. In Intelligent Robotics and Applications: 9th International Conference, ICIRA 2016, Tokyo, Japan, August 22-24, 2016, Proceedings, Part I 9 (pp. 134-146). Springer International Publishing.

[9] Luo, C., and Zhang, W. (2019). VGS hand: A novel hybrid grasping modes robot hand with variable geometrical structure. Applied Sciences, 9(8), 1566.

[10] Xu, J., Liang, W., Cai, J., Yuan, C., Yang, P., Zeng, B., and Zhang, W. (2017, August). LPSA underactuated mode of linearly parallel and self-adaptive grasping in the CLIS robot hand with Chebyshev linkage and idle stroke. In 2017 2nd International Conference on Advanced Robotics and Mechatronics (ICARM) (pp. 322-327). IEEE.

[11] Hu, J., Li, K., Zhang, W., Xu, X., and Rodic, A. (2017). LIPSAY Hand: A linear parallel and self-adaptive hand with y-shaped linkage mechanisms. In Intelligent Robotics and Applications: 10th International Conference, ICIRA 2017, Wuhan, China, August 16–18, 2017, Proceedings, Part II 10 (pp. 739-751). Springer International Publishing.

[12] Liu, Y., and Zhang, W. (2019, August). An Underactuated Robot Finger with Movable Skeleton Link and Hoeckens Mechanism for Linear Clamping and Self-adaptive Grasping. In 2019 IEEE International Conference on Real-time Computing and Robotics (RCAR) (pp. 562-567). IEEE.

[13] Luo, C., and Zhang, W. (2019). VGS hand: A novel hybrid grasping modes robot hand with variable geometrical structure. Applied Sciences, 9(8), 1566.

[14] Yang, Y., Zhang, W., Xu, X., Hu, H., and Hu, J. (2017). LIPSA hand: a novel underactuated hand with linearly parallel and self-adaptive grasp. In Mechanism and Machine Science: Proceedings of ASIAN MMS 2016 and CCMMS 2016 (pp. 111-119). Springer Singapore.